CHEMICAL ENGINEERING TRANSACTIONS
VOL. 100, 2023
A publication of AIDIC
The Italian Association of Chemical Engineering
Online at www.cetjournal.it
Guest Editors: Sauro Pierucci, Flavio Manenti

ISBN 979-12-81206-03-8; **ISSN** 2283-9216
DOI: 10.3303/CET23100073

The Effect of Composition and Heat Treatment on Microhardness of Ni-P and Ni-P-nanoZrO_2 Coatings

Giulia Pedrizzetti*, Laura Paglia, Virgilio Genova, Marco Conti, Lidia Baiamonte, Francesco Marra

Dept. of Chemical Engineering Materials Environment, Sapienza University of Rome, INSTM Reference Laboratory for Engineering of Surface Treatments, Via Eudossiana 18, Rome, Italy
giulia.pedrizzetti@uniroma1.it

Electroless Ni-P coatings have widespread industrial usage and their composition can be tailored by the introduction of hard ceramic nanoparticles, to create a nanocomposite coating with improved properties. In this work, nanoZrO_2 reinforced Ni-P coating with medium P content (MP, ~6 wt.%) and high P content (HP, ~11 wt.%) were produced and heat treated at 200°C, 340°C, 400°C and 600°C, to study the evolution of microstructure and microhardness properties as a function of coating composition and annealing temperature. Results demonstrated that introducing ZrO_2 nanoparticles efficiently increases the hardness of both MP and HP nanocomposites without altering their microstructure, either in the as-deposited state or after heat treatments. Conversely, P content strongly affects microstructure and crystallization behavior upon heat treatments: nanocrystalline MP coatings experience Ni_3P precipitation with treatment at 340°C, with subsequent controlled grain growth, whereas amorphous HPs undergo crystallization and Ni_3P precipitation after treatment at 400°C. Microhardness evolution according to microstructural changes was evaluated and both coatings exhibited the highest HV_{50} values after treatment at 400°C, at which complete Ni_3P precipitation is achieved. Microhardness of nanocomposite coatings is always higher than particle-free ones, demonstrating that the synergistic effect of dispersion hardening (given by nano-ZrO_2) and precipitation strengthening (given by Ni_3P) can be an effective method to improve properties and meet the demanding need of engineering applications.

1. Introduction

Electroless Nickel-Phosporus coatings have extensive applications in many industrial fields of engineering to protect components from extreme environmental attack (Kundu et al., 2019). Thanks to their excellent properties of corrosion and wear resistance, hardness and solderability, Ni-P coatings gained much interest as a valid alternative to traditional commercial Cr-based electrodeposited coatings.
Finding a reasonable substitute to hard chrome plating has become an urgent need for industrial development, since the well-established deposition baths containing Cr(VI) have been limited in the context of REACH regulation: its hazardous nature, being carcinogenic, corrosive and strongly oxidizing, imposes health, safety and environmental concerns (Alfort, 2017). Yet, deposition from the newly proposed Cr(III) baths from aqueous solutions remains a challenge. Despite being a more environmentally friendly alternative, the high stability of Cr(III) complex with water molecules and the considerable hydrogen evolution at the cathode, which in turn results in the formation of inert compounds, considerably limits the maximum thickness of the coating, that is generally lower than 10 µm and makes the product unsuitable for functional applications (Adachi et al., 2020; Xu et al., 2020). Therefore, much attention is focused on finding alternatives to Cr deposition that can maintain the excellent properties required for engineering applications. Extensive studies have shown that Ni-P coating can offer adaptive solutions to a wide range of environmental and working conditions (Lelevic and Walsh, 2019). In particular, Ni-P coatings have a widespread application in the energy production industry, to protect rotor and stator components of compressors from many degradation phenomena that would invariably deteriorate their performance, including corrosion, erosion and wear. The strategic application of Ni-P coatings can mitigate surface degradation of materials and increase service life of components.

Paper Received: 12 January 2023; Revised: 25 April 2023; Accepted: 25 May 2023
Please cite this article as: Pedrizzetti G., Paglia L., Genova V., Conti M., Baiamonte L., Marra F., 2023, The Effect of Composition and Heat Treatment on Microhardness of Ni-P and Ni-P-nanoZrO_2 Coatings, Chemical Engineering Transactions, 100, 433-438 DOI:10.3303/CET23100073

The electroless plating process allows the controlled reduction of metal ions onto a catalytic substrate by the incorporation of a reducing agent in the plating solution (Genova et al., 2019). No external current is needed and uniform coatings can be obtained on any surface, regardless of its shape (Genova et al., 2017). Incorporation of phosphorus in the Ni matrix affects the structure and properties of coatings: high P coatings (HP, 10-13 wt.%) are amorphous and highly corrosion resistant, whereas medium P coatings (MP, 6-9 wt.%) are nanocrystalline and characterized by higher hardness and wear resistance (Balaraju et al., 2006). Hardness of Ni-P coatings can be increased by thermal treatments, which induce phase transformation and precipitation of Ni_3P hard phases. Nevertheless, crystallization may also induce the formation of micro-cracks, that negatively affect corrosion resistance (Ahmadkhaniha et al., 2018). Another strategy to increase hardness of Ni-P deposits without altering the microstructure consists of the introduction of nanosized hard particles, to create a nanocomposite coating with improved properties. Among the ceramic particles proposed as the reinforcing phase, nano-ZrO_2 has gained much interest thanks to its good mechanical properties and high ζ-potential, which guarantees low agglomeration and ease of incorporation (Chinchu et al., 2020; Shibli et al., 2019; Zielińska et al., 2012). In this work, Ni-P and Ni-P-nanoZrO_2 coatings with medium and high P content are produced with an original lead-free solution and annealed at different temperatures, to provide a comparative study on the combined effect of composition and microstructural evolution on microhardness properties.

2. Materials and methods

Squared specimens of ASTM 182 F22 steel with dimensions of 15 mm x 15 mm x 3 mm were selected as substrates. All chemicals were of analytic grade and purchased by Alfa Aesar (Thermo Fisher Scientific).

2.1 Coating preparation

Samples were sandblasted with corundum (mesh 80) as abrasive material, to remove contaminants and increase surface roughness, which promotes deposition. Just before immersion in the plating bath, acidic pickling of substrates with 50 vol.% diluted solution of HCl 37% was performed for 1 minute at room temperature, to remove any trace of surface oxides. Rinsing in deionized water was performed after each cleaning step. Composition of the lead-free electroless solutions for MP and HP deposition is reported in Table 1.

Table 1: Composition of the plating solutions for deposition of MP and HP.

Compound	Function	Amount for MP [g/L]	Amount for HP [g/L]
Sodium hypophosphite	Reducing agent	70	110
Sodium acetate	Buffer	15	20
Citric acid	Chelating Agent	6	9
Nickel sulphate	Source of Nickel	12	25
Thio-organic compound	Stabilizer*	5 ppm*	8.5 ppm*

*The stabilizer was added by liquid solution (1 mol/kg) and respecting the quantity in ppm.

Commercial ZrO_2 nanoparticles, with an average particle size of 50-100 nm, were purchased from Io-Li-Tec (Ionic Liquid Technologies GmbH) and used without any further purification. Previous experimental activities demonstrated that introduction of 13.5 g/L of nanoparticles allowed the best compromise between incorporation in the coating and agglomeration. Weighted powders were added to aqueous solutions and sonicated with Elmasonic S 30 (H) ultrasonic cleaning unit for at least 15 minutes, to promote dispersion, before adding them to the plating solution. Depositions of both MP and HP particle-free and nanocomposite coatings were performed at 90°C for 90 minutes, under continuous magnetic stirring and constant control over temperature.
The study of microstructural evolution upon exposure at high temperature was carried out performing isothermal heat treatments at 200°C, 340°C, 400°C and 600°C for 1 hour. All treatments were performed in air in a Lenton tube furnace (now Carbolite Gero Ltd.). The presence of through-the-thickness cracks and defects induced by thermal exposure was investigated by the Ferroxyl reagent test (ASTM B689-97).

2.2 Coating Characterization

Surface morphology and composition of the coatings were determined with a FEG-SEM Tescan Mira3 (Tescan, Brno, Czech Republic) equipped with Edax Octane Elect detector for energy-dispersive X-Ray spectroscopy (EDS). X-ray diffraction analysis (XRD) was performed with a Philips X'Pert diffractometer (PANalytical BV, The Netherlands), operating at 40 KV and 40 mA with CuKα1 radiation, with scan range of 20–80° (2θ), feed step of 0.02° and acquisition time of 2 s. The microstructural characteristics of standard and nanocomposite coatings were investigated as a function of phosphorus content and temperature of heat treatment. The crystallite size was calculated using Scherrer's equation (1):

$$D = \frac{0.94\lambda}{\beta \cos(\theta)}, \quad (1)$$

where λ is the wavelength of the radiation used, β is the half-maximum width and θ is the position of the main peak. No correction for instrumental broadening was made.
Microhardness of the coatings was evaluated according to ASTM E384-11 using a Leica VMHT (Leica GmbH) with a Vickers diamond indenter, with 50 gf load condition and indentation time of 15 seconds. Distance between two indentations was ≥50 μm, results report the average value and standard deviation of at least twenty repeated measurements.

3. Results and discussion

Surface morphology of HP and MP coatings reinforced with nano-ZrO_2 and its evolution as a function of heat treatment temperature is reported in Figure 1. Both coatings show the typical cauliflower-like morphology of electroless NiP layers and some ZrO_2 can be observed on the Ni-P surface. As expected, deposits with high P content exhibit smaller nodular size compared with MP ones, since the higher P content limits the lateral growth of nodules and promotes nucleation phenomena. MP nanocomposite annealed at 340°C and 400°C for 1h have similar morphology, with finer micronodular structure compared with those treated at 200°C. In HP nanocomposites, a similar nodular refinement can only be observed after heat treatment at 400°C, whereas annealing at 340°C does not induce morphological changes. After exposure at 600°C, an oxide scale is visibly starting to grow at the surface of both types of coatings, giving a porous and sponge-like structure. Similar results about morphology refinement after heat treatments above the crystallization temperature are described in literature (Chinchu et al., 2020; Karthikeyan et al., 2016). Therefore, the different temperature at which smaller spherical nodules form between MP and HP nanocomposites suggests a different crystallization behavior depending on the P content.

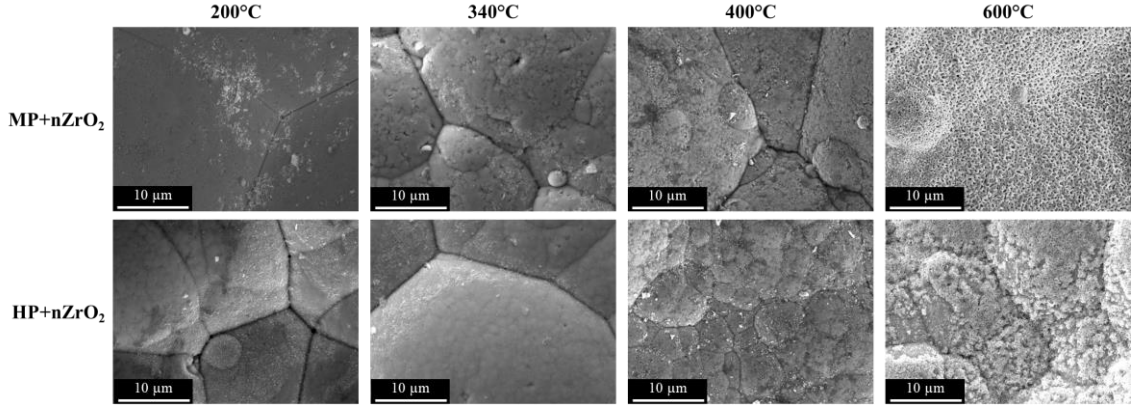

Figure 1: SEM micrographs showing morphology evolution of MP and HP nanocomposite coatings according to the different temperature of heat treatment.

To uncover this aspect, microstructural evolution was investigated via XRD analysis. Comparison of XRD spectra of as-deposited ZrO_2-reinforced MP and HP coatings is reported in Figure 1(a). EDS analysis demonstrated that HP nanocomposites contain ~11 wt.% of P, which is sufficient to produce an amorphous Ni-P alloy. In this case, only one broad peak of Ni (111) is detectable in the XRD spectrum. Conversely, MP coatings, with P content ~6 wt.%, are characterized by a nanocrystalline microstructure and XRD analysis reveals the presence of additional Ni (200) and Ni (220) peaks. ZrO_2 peaks can be identified in both spectra, confirming the presence of nanoparticles.
Figures 1(b) and (c) show, respectively, the structural evolution of MP and HP nanocomposites as a function of heat treatment temperature. The heat treatment at 200°C is necessary as dehydrogenation process: since Ni-P deposition occurs along with H_2 generation, this gas inevitably remains entrapped in the coating, causing embrittlement and formation of porosities (Wang et al., 2011); dehydrogenation is therefore required to avoid a dramatical reduction of mechanical properties. Since the crystallization temperature of Ni-P deposits is reported to be around 340°C(Huang et al., 2003), aging at 200°C does not induce phase transformation and the microstructure of both types of coatings remains similar to the as-coated condition. When the heat treatment is performed at 340°C, a different microstructure between MP and HP deposits is observed: in MP coatings, crystallization and precipitation of Ni_3P phase occurs, whereas HP remains amorphous and no compounds other than Ni are detected. This dissimilar behavior can be explained considering that exposure to high temperature

leads to two main effects: (*i*) grain growth of the Ni matrix and (*ii*) phosphorus segregation at grain boundaries and triple junctions, with consequent formation of P-rich regions. Crystallization of the MP nanocomposite after exposure at 340°C for 1h suggests that the initial nanocrystalline structure provides a higher number of sites for P segregation, with a higher probability to exceed the threshold necessary for Ni_3P precipitation (reported to be close to the eutectic concentration, ~11 wt.% of P (Farber et al., 2000)). It was proposed that the structural changes that occur with temperature increase develop through the formation of a metastable grain boundary phase, given by a supersaturated solid solution of phosphorus in nickel (Hentschel et al., 2000). In HP coatings, this phase already develops in the as-deposited state due to the higher P content, giving it more thermal stability at low temperature. Therefore, full crystallization of the amorphous HP nanocomposites is only obtained after the treatment at 400°C. These results can also explain the differences observed in the morphological analysis. After treatment at 600°C, the relative intensity of peaks increases and both spectra become sharper. Ni grain growth and coalescence of Ni_3P precipitates take place without the formation of other new phases, confirming that the introduced ZrO_2 nanoparticles are chemically inert and do not affect phase composition of the coatings. The presence of nickel oxide peaks at 600°C should also be highlighted, confirming the growth of a thin oxide scale.

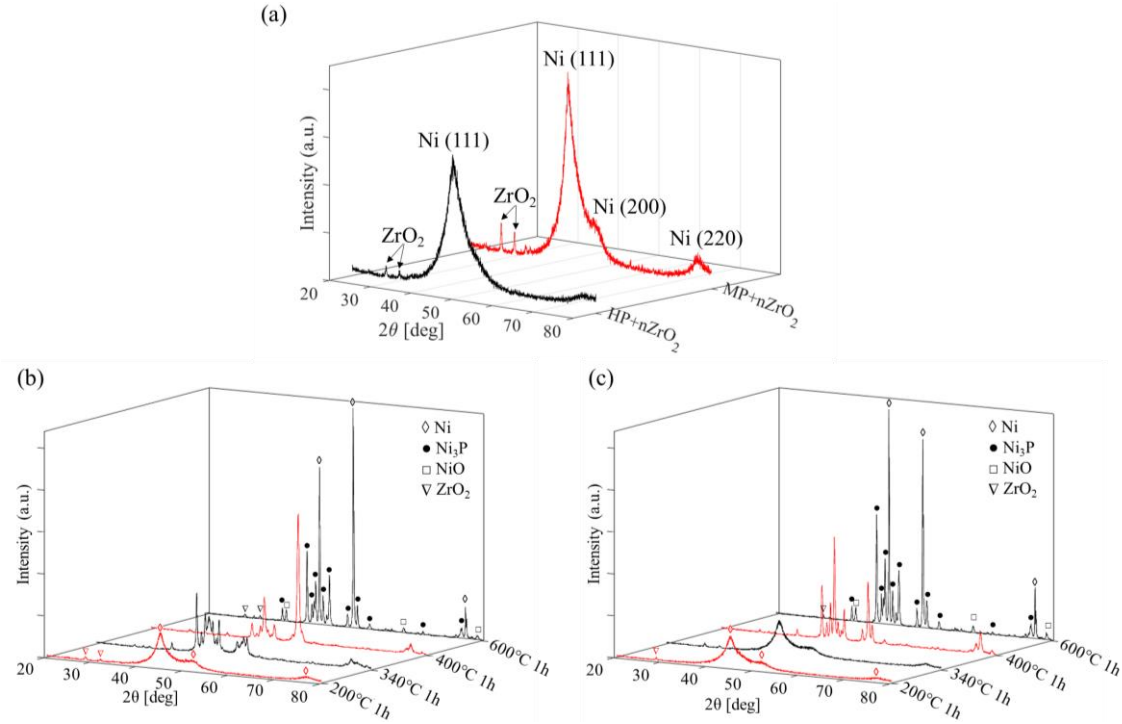

Figure 2: (a) XRD spectra of HP and MP nanocomposites in the as-deposited condition; (b) XRD spectra of MP nanocomposite coatings after 1h heat treatment at different temperature; (c) XRD spectra of HP nanocomposite coatings after 1h heat treatment at different temperature.

Comparison of spectra at 400°C also reveals that HP coatings have sharper Ni and Ni_3P peaks compared with MP, which indicate higher grain size of Ni crystallites and precipitates. Evolution of average grain size, calculated with Scherrer equation (eq. 1), and coarsening of Ni_3P precipitates with increasing heat treatment temperature is reported in Figure 3. Grain size of MP nanocomposite coatings is coarser than HP for heat treatment temperature up to 340°C, where the latter still exhibit an amorphous microstructure. The trend is inverted at 400°C, where HP coatings exhibit coarser grains, indicating higher thermal stability of coatings with medium P content when temperature is increased. This is explained considering that in MP deposits the heat treatment at 340°C temperature induces initial Ni_3P precipitation: a metastable thermodynamic equilibrium is developed between the Ni alloy and the P-enriched grain boundary phase, so that substantial grain growth is only possible with additional formation of Ni_3P, which acts a sink for P atoms (Farber et al. 2000). Moreover, increase in Ni crystallite size is further restrained by the presence of the small precipitates themselves, due to the drag mechanism. Conversely, in HP coatings the metastable equilibrium is already present in the as-deposited state and, despite the higher thermal stability at low temperature, at higher temperature P segregation is more likely to exceed the threshold for massive Ni_3P precipitation, allowing major grain growth to occur (Hentschel et al., 2000). At 600°C, precipitation is probably complete and both coatings exhibit a comparable structure.

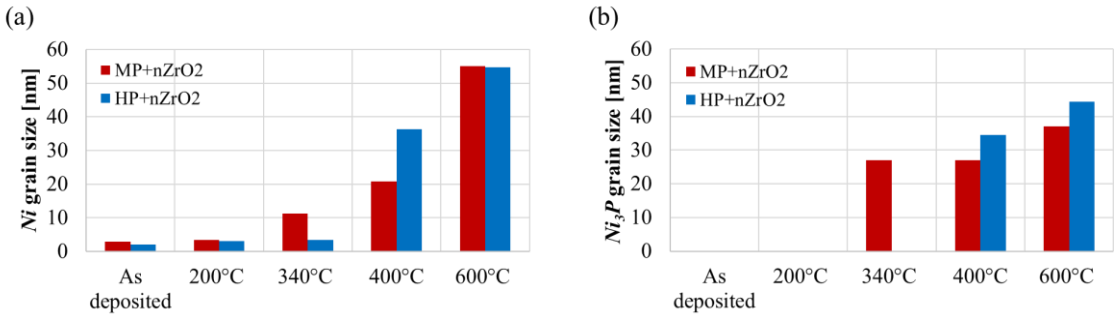

Figure 3: Increase of average nickel crystallite size (a) and coarsening of Ni3P precipitates (b) with increasing annealing temperature for MP and HP coatings reinforced with nano-ZrO_2.

Both MP and HP standard and nanocomposite coatings after heat treatments are successfully tested to Ferroxyl reagent test, indicating that neither nanoparticle introduction nor crystallization and phase change induce the formation of through-the-thickness defects, which could prejudice mechanical properties and corrosion resistance. Since microstructural changes induced by heat treatments are often exploited to modify coating properties, Figure 4 shows microhardness of particle-free and nanocomposite coatings in the as-deposited condition and after annealing at the different investigated temperatures. The synergistic effect between nanoparticles introduction and microstructural features on coating microhardness results in higher HV_{50} values for nanocomposites compared with their standard counterpart, with a progressive hardness increase up to treatment at 400°C. Dispersion hardening effect given by hard nanoparticles introduction effectively strengthens coatings, thanks to the simultaneous action as a barrier to dislocation motion, according to Orowan mechanism, and the load-bearing effect (Zhang and Chen, 2008).
Both MP standard and nanocomposites have higher hardness than HP ones because deformation processes in NiP coatings with very small grain size (between 2 nm and 15 nm) are governed by grain boundary sliding and rotation, according to the *reverse* Hall-Patch effect (Apachitei et al., 2002); therefore, higher size of crystallites, which associates with a lower amount of grain boundaries, results in enhanced microhardness. Above 340°C, initial Ni_3P precipitation in MP coatings further enhances hardness. In fact, the small and semi-coherent precipitates are an additional barrier to dislocation motion, which have to move through the hard Ni_3P to cause deformation. Precipitation in MP coatings seems to be not yet complete after treating at 400°C, which results in additional hardening at 400°C. Maximum hardness for HP coatings is also reached at 400°C, when, according to XRD analysis, crystallization and precipitation occur. At 600°C, both coatings show lower hardness due to excessive grain growth and coalescence of precipitates. These results are in agreement with those reported by other authors in similar studies, where hardness decrease is registered after treatment at 600°C (Amjad-Iranagh and Zarif, 2020; Jiang et al., 2016). Indeed, beyond the threshold of 15 nm, higher grain size corresponds to lower hardness, in accordance with the Hall-Patch equation, and larger precipitates make it easier for dislocations to loop around them, leading to a less effective Orowan strengthening.

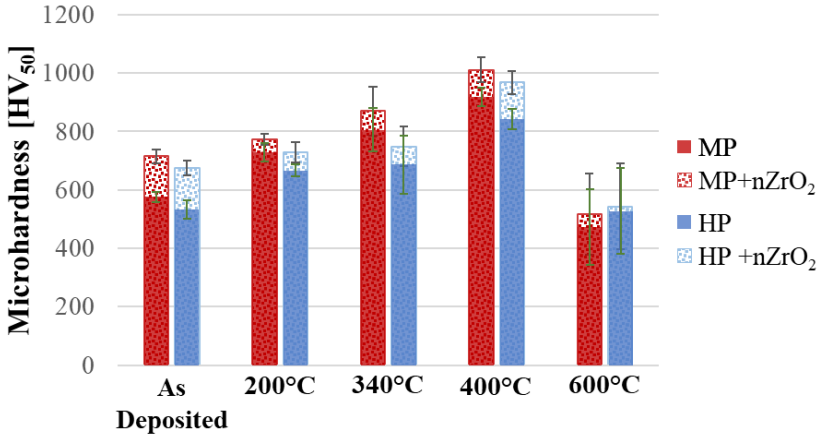

Figure 4: Comparison of microhardness (HV) between particle-free and ZrO_2-reinforced MP and HP coatings in the as-deposited condition and after heat treatment at 200°C, 340°C, 400°C and 600°C for 1 h in air.

4. Conclusions

Electroless Ni-P-ZrO_2 nanocomposite coatings with medium and high P content are successfully produced and characterized. Introduction of the reinforcing phase led to a hardness increase by ~22% and ~24% for nanocrystalline MP and amorphous HP coatings, respectively, without altering their microstructure in the as-deposited state. A different crystallization behavior was observed for MP and HP coatings, which can be ascribed to the different P content. ZrO_2 demonstrated to be chemically inert to the Ni-P deposit and does not alter phase composition upon heat treatments. Precipitation of the intermetallic Ni_3P starts at 340°C in MP coatings, whereas can only be observed after treatment at 400°C for HP coatings. Maximum hardness, up to 1012 HV_{50} for MP and 968 HV_{50} for HP nanocomposites, is obtained after treatment at 400°C, due to the synergistic effect of nanoparticles dispersion hardening and Ni_3P precipitation strengthening.

Reference

Adachi, K., Kitada, A., Fukami, K., Murase, K., 2020. Crystalline chromium electroplating with high current efficiency using chloride hydrate melt-based trivalent chromium baths. Electrochim Acta 338.

Ahmadkhaniha, D., Eriksson, F., Leisner, P., Zanella, C., 2018. Effect of SiC particle size and heat-treatment on microhardness and corrosion resistance of NiP electrodeposited coatings. J Alloys Compd 769, 1080–1087.

Alfort, H.-J., 2017. When Does the Ban on Chromium (VI) Come into Effect? International Surface Technology 1, 48–51.

Amjad-Iranagh, S., Zarif, M., 2020. TiO2 nano-particle effect on the chemical and physical properties of Ni-P-TiO2 nanocomposite electroless coatings. Journal of Nanostructures 10, 415–423.

Apachitei, I., Tichelaar, F.D., Duszczyk, J., Katgerman, L., 2002. The effect of heat treatment on the structure and abrasive wear resistance of autocatalytic NiP and NiP-SiC coatings. Surf Coat Technol 149, 263-278.

Balaraju, J.N., Sankara Narayanan, T.S.N., Seshadri, S.K., 2006. Structure and phase transformation behaviour of electroless Ni-P composite coatings. Mater Res Bull 41, 847–860.

Chinchu, K.S., Riyas, A.H., Ameen Sha, M., Geethanjali, C. v., Saji, V.S., Shibli, S.M.A., 2020. ZrO2–CeO2 assimilated electroless Ni–P anti-corrosion coatings. Surfaces and Interfaces 21.

Farber, B., Cadel, E., Menand, A., Schmitz, G., Kirchheim, R., 2000. Phosphorus segregation in nanocrystalline Ni 3.6 at.% P investigated with the Tomographic Atomic Proble (TAP). Acta Mater 48, 789–796.

Genova, V., Marini, D., Valente, M., Marra, F., Pulci, G., 2017. Nanostructured nickel film deposition on carbon fibers for improving reinforcement-matrix interface in metal matrix composites. Chem Eng Trans 60, 73–78.

Genova, V., Paglia, L., Marra, F., Bartuli, C., Pulci, G., 2019. Pure thick nickel coating obtained by electroless plating: Surface characterization and wetting properties. Surf Coat Technol 357, 595–603.

Hentschel, T.H., Isheim, D., Kirchheim, R., Mu, F., Ller, È., Kreye, H., 2000. Nanocrystalline Ni 3.6 at.% and its tranformation sequence studied by atom-probe field-ion microscopy. Acta Mater 48, 933–941.

Huang, Y.S., Zeng, X.T., Annergren, I., Liu, F.M., 2003. Development of electroless NiP-PTFE-SiC composite coating. Surf Coat Technol 167, 207–211.

Jiang, J., Chen, H., Zhu, L., Qian, W., Han, S., Lin, H., Wu, H., 2016. Effect of heat treatment on structures and mechanical properties of electroless Ni-P-GO composite coatings. RSC Adv 6, 109001–109008.

Karthikeyan, S., Vijayaraghavan, L., Madhavan, S., Almeida, A., 2016. Study on the Mechanical Properties of Heat-Treated Electroless NiP Coatings Reinforced with Al2O3 Nano Particles. Metall Mater Trans A Phys Metall Mater Sci 47, 2223–2231.

Kundu, S., Das, S.K., Sahoo, P., 2019. Friction and wear behavior of electroless Ni-P-W coating exposed to elevated temperature. Surfaces and Interfaces 14, 192–207. https://doi.org/10.1016/j.surfin.2018.12.007

Lelevic, A., Walsh, F.C., 2019. Electrodeposition of Ni-P alloy coatings: A review. Surf Coat Technol 369, 198–220.

Shibli, S.M.A., Chinchu, K.S., Sha, M.A., 2019. Development of Nano-tetragonal Zirconia-Incorporated Ni–P Coatings for High Corrosion Resistance. Acta Metallurgica Sinica (English Letters) 32, 481–494.

Wang, L.L., Chen, H.J., Chen, Z.L., 2011. Study on post-treatments for electroless Ni-P coating. Surface Engineering 27, 57–60.

Xu, L., Pi, L., Dou, Y., Cui, Y., Mao, X., Lin, A., Fernandez, C., Peng, C., 2020. Electroplating of Thick Hard Chromium Coating from a Trivalent Chromium Bath Containing a Ternary Complexing Agent: A Methodological and Mechanistic Study. ACS Sustain Chem Eng 8, 15540–15549.

Zhang, Z., Chen, D.L., 2008. Contribution of Orowan strengthening effect in particulate-reinforced metal matrix nanocomposites. Materials Science and Engineering A 483–484, 148–152.

Zielińska, K., Stankiewicz, A., Szczygieł, I., 2012. Electroless deposition of Ni-P-nano-ZrO 2 composite coatings in the presence of various types of surfactants. J Colloid Interface Sci 377, 362–367.